Aurantiamide-related dipeptide derivatives are formyl peptide receptor 1 antagonists

Journal:	*RSC Medicinal Chemistry*
Manuscript ID	MD-RES-06-2019-000336.R2
Article Type:	Research Article
Date Submitted by the Author:	30-Sep-2019
Complete List of Authors:	Mastromarino, Margherita; Università degli Studi di Bari Aldo Moro, Dipartimento di Farmacia - Scienze del Farmaco Kirpotina, Lilya; Montana State University Bozeman, Department of Microbiology and Immunology Schepetkin, Igor A.; Montana State University Bozeman, Department of Microbiology and Immunology Quinn, MT; Montana State University Bozeman, Department of Microbiology and Immunology Lacivita, Enza; Università degli Studi di Bari Aldo Moro, Dipartimento di Farmacia-Scienze del Farmaco Leopoldo, Marcello; Università degli Studi di Bari Aldo Moro, Dipartimento di Farmacia - Scienze del Farmaco

Aurantiamide-related dipeptide derivatives are formyl peptide receptor 1 antagonists

Margherita Mastromarino,[1] Liliya N. Kirpotina,[2] Igor A. Schepetkin,[2] Mark T. Quinn,[2] Enza Lacivita*,[1] and Marcello Leopoldo[1]

[1]Dipartimento di Farmacia - Scienze del Farmaco, Università degli Studi di Bari Aldo Moro, via Orabona, 4, 70125 Bari, Italy

[2]Department of Microbiology and Immunology, Montana State University, Bozeman, MT 59717, United States

*Corresponding Author: Enza Lacivita, Dipartimento di Farmacia – Scienze del Farmaco, Università degli Studi di Bari "A. Moro", via Orabona, 4, 70125, Bari, Italy. E-mail: enza.lacivita@uniba.it; Phone: +39 080 5442750; Fax: +39 080 5442231

Abstract

Formyl peptide receptor 1 (FPR1) is expressed on a variety of immune system cells and is a key regulator of the inflammatory environment. Therefore, the development of FPR1 antagonists may represent a novel approach for modulating innate immunity and treating inflammatory diseases. Starting from a dipeptide scaffold that is structurally related to the natural product aurantiamide, we investigated the structure-activity relationships of the dipeptide (2*R*,2'*S*)-**6**, which was reported as an FPR1 antagonist. We found that the absolute configuration *2R,2'S* was preferred to obtain potent and selective FPR1 antagonists. The structural modifications performed on the terminal fragments of the molecule suggest that the size of the substituents can greatly influence the interaction with FPR1. These compounds behaved as antagonists in human neutrophils and were able to inhibit formyl peptide-induced chemotaxis. Since FPR1 is a key regulator of the inflammatory environment, the dipeptide derivatives described here may represent important leads for the development of new potent and selective FPR1 antagonists for the treatment of neutrophil-mediated inflammatory diseases.

Introduction

Inflammation is associated with a wide variety of diseases, and a hallmark of inflammation is leukocytes infiltration in response to pathogen- or damage-associated chemotactic molecular patterns. Physiological and pathological trafficking of leukocytes is mediated by the interaction of chemotactic molecular patterns with multiple G-protein coupled receptors (GPCR).[1] Among the chemotactic GPCRs, formyl peptide receptors (FPRs) play an important role in leukocyte activation and chemotaxis.[2] FPRs are mainly expressed in leukocytes, including neutrophils, monocytes/macrophages, natural killer cells, and dendritic cell.[2,3] However, FPRs are also expressed in a variety of non-immune cells, such as endothelial cells, bone marrow-derived mesenchymal stem cells, and hepatocytes, suggesting a broader spectrum for biological function of these receptors.[2,3] In humans, there are three FPR subtypes, named FPR1, FPR2, and FPR3. FPR1 was originally identified as a receptor for *N*-formyl peptides, which are produced by bacteria or can be released from damaged mitochondria during tissue injury.[2,4] In neutrophils, FPR1 activation induces chemotaxis, production of superoxide anions, Ca^{2+} mobilization and cytokine release .[3,5] FPR1 has been reported to contribute to the pathogenesis of several diseases. For example, FPR1 expression is correlated with tumor progression and survival in gastric cancer.[6] In human hepatocellular carcinoma cells, FPR1 mediates tumorigenicity by promoting the inflammatory response.[7] FPR1 is selectively expressed by highly malignant human glioma cells where it regulates motility, growth, and the production of angiogenic factors, in part by transactivation of the epidermal growth factor receptor (EGFR).[8,9] High expression of FPR1 in neuroblastoma primary tumors corresponds with high-risk disease and poor patient survival.[10] FPR1 is also involved in the inflammatory aspects of other physiological and pathological processes, such as modulation of platelet activation and thrombus formation.[11] Blockade of FPR1 can be useful in hepatic ischemia-reperfusion injury[12] and may have protective effects in acute lung injury.[13] On the basis of such evidence, FPR1 antagonists might be useful in host defense in order to reduce detrimental effects

associated with inflammation and cancer, supporting the search for FPR1 antagonists with tissue-protective effects.

The most potent and receptor-specific FPR1 antagonists described so far are the fungal hydrophobic cyclic peptides, cyclosporines A and H, which are able to block *f*MLF-induced analgesia *in vivo*.[14,15] However, considering the biological profiles of these compounds, it cannot be ruled out that part of the effects observed *in vivo* may not be FPR1-mediated. Several "small-molecule" FPR1 antagonists exhibiting a wide range of antagonist potency and selectivity towards FPR2 have been identified so far (for extensive review see ref.16), including the diamide derivatives exemplified by compound **1**,[17] the pyrazole-4-carboxamides like compound **2**,[18] the methionine-derived benzimidazoles (compound **3**),[17] the 4*H*-chromen-4-one derivatives, exemplified by compound **4**,[19] and the 1*H*-pyrrol-2(5*H*)-one derivatives such as compound **5**[20] (Figure 1). In the search for new molecular scaffolds that could be easily optimized further, several natural products have been screened in order to identify compounds endowed with FPR1 antagonist activity.[21] Among these is aurantiamide acetate (Figure 2), a natural product isolated from several species, including *Polygonum chinensin*[22] and *Aspergillus penicilloides*.[23]

Aurantiamide acetate is a dipeptide obtained from condensation of benzoylphenylalanine with phenylalaninol, which shows anti-inflammatory properties *in vitro* by inhibiting nitric oxide (NO) and prostaglandin E_2 release in RAW 264.7 cells stimulated with the bacteria endotoxin lipopolysaccharide (LPS).[24] Similarly, in human microglial BV-2 cells stimulated with LPS, aurantiamide acetate was able to attenuate inducible NO synthase (iNOS), cyclooxygenase-2 (COX-2), and pro-inflammatory cytokines, such as interleukin-1β (IL-1β) and tumor necrosis factor (TNF), suggesting neuroprotective properties.[25] A study by Hwang et al[26] has reported the structure-activity relationships of a series of dipeptides structurally related to aurantiamide acetate, exemplified by compounds (2*R*,2'*S*)-**6** and (2*R*,2'*S*)-**7** (Figure 2) which had anti-inflammatory properties. In fact, both compounds were able to potently inhibit $O_2^{\bullet-}$ generation and neutrophil elastase release in neutrophils stimulated by the potent FPR1 agonist *f*MLF suggesting that the anti-

inflammatory effects of compounds (2*R*,2'*S*)-**6** and (2*R*,2'*S*)-**7** are mediated through the interaction with FPR1. The molecular scaffold of aurantiamide acetate and related analogues is attractive because it offers the possibility of optimizing the biological profile through modification of the amino acid residues. Therefore, we embarked in a program to explore the structure-activity relationships of dipeptidyl derivatives with the aim of developing "drug-like" FPR1 antagonists.

Study design

As stated above, the dipeptidyl scaffold is attractive for the development of FPR1 antagonists because it can be easily modified. However, it may show some limitations in pharmacokinetic properties. Therefore, we synthesized aurantiamide acetate and compounds (2*R*,2'*S*)-**6** and (2*R*,2'*S*)-**7**, according reported methods,[26] and we tested them for their susceptibility to oxidative metabolism *in vitro* using rat liver microsomes. Furthermore, we confirmed the antagonist properties by assessing their effect on Ca^{2+} mobilization in HL60 cells stably expressing FPRs and primary human neutrophils.

Microsomal stability was assessed as the percentage of recovery of parent compound after a 30 min incubation with liver microsomes in the presence of an NADPH-regenerating system, as described previously.[27] We found that aurantiamide acetate was chemically unstable in the incubation medium, whereas compound (2*R*,2'*S*)-**6** and (2*R*,2'*S*)-**7** showed 24% and 10% recovery of the parent compound, respectively. Thus, we selected only compounds (2*R*,2'*S*)-**6** and (2*R*,2'*S*)-**7** for further studies.

We tested the effects of compounds (2*R*,2'*S*)-**6** and (2*R*,2'*S*)-**7** on Ca^{2+} mobilization in HL60 cells stably transfected with FPR1 or FPR2 to assess which FPR subtype was responsible of the reported anti-inflammatory properties[26] and selectivity (Table 1). We found that none of the compounds was able to induce Ca^{2+} mobilization in either FPR1- or FPR2-HL60 cells, suggesting that the compounds were not able to activate FPR1 or FPR2. In contrast, both compounds dose-dependently blocked Ca^{2+} mobilization induced by the agonist *f*MLF in FPR1-HL60 cells, but they did not block

the effect of the selective FPR2 agonist WKYMVM in FPR2-HL60 cells (Table 1). These data clearly indicated that compounds (2*R*,2'*S*)-**6** and (2*R*,2'*S*)-**7** are potent and selective FPR1 antagonists. Based on metabolic stability and Ca^{2+} mobilization data, we selected compound (2*R*,2'*S*)-**6** for further structural modifications. Since compound (2*R*,2'*S*)-**6** has two stereocenters, we first explored which absolute configuration was preferred for interaction with FPR1. We then we modified both ends of the molecule. For all compounds the effect on Ca^{2+} mobilization in both FPR1- and FPR2-HL60 cells was assessed.

Chemistry

The targets compounds have been synthesized as depicted in Schemes 1 and 2. The four stereoisomers of compound (2*R*,2'*S*)-**6** were prepared by condensing (*R*)- or (*S*)-phenylalanine methyl ester with (*R*)- or (*S*)-Boc tryptophan after activation with *N-N'*-carbonyldiimidazole to obtain the derivatives (2*R*,2'*S*)-**8**, (2*S*,2'*R*)-**8**, (2*S*,2'*S*)-**8**, and (2*R*,2'*R*)-**8**. Subsequently, these latter compounds were deprotected with trifluoroacetic acid to obtain the amines (2*R*,2'*S*)-**9**, (2*S*,2'*R*)-**9**, (2*S*,2'*S*)-**9**, and (2*R*,2'*R*)-**9**. These intermediates were then condensed with benzoic acid after activation with *N-N'*-carbonyldiimidazole to obtain the desired target compounds.

The final compounds **10** and **11** (Scheme 2), in which the phenyl ring of the benzoyl group was replaced with alkyl residues, were prepared by condensing the amine (2*R*,2'*S*)-**9**, which was obtained as described above, with cyclohexanecarboxylic acid and isovaleric acid, respectively, previously activated with *N-N'*-carbonyldiimidazole. The final compounds **12** and **13**, formally derived from compound (2*R*,2'*S*)-**6** by replacing phenylalanine with leucine and valine, respectively, were prepared according to Scheme 2. The (*S*)-Boc tryptophan was activated with *N-N'*carbonyldiimidazole and condensed with (*R*)-leucine methyl ester to obtain the Boc-protected derivative **14**, whereas the Boc-protected derivative **15** was prepared by activating (*S*)-Boc tryptophan with PyBOP in the presence of N-methylmorpholine and then condensing with (*R*)-valine methyl ester. The derivatives **14** and **15** were deprotected with trifluoroacetic acid to obtain

the amines **16** and **17**, respectively, which were condensed with benzoic acid after activation with *N-N'*-carbonyldiimidazole to obtain the desired target compounds **12** and **13**.

Results and Discussion

The effects of the new compounds on Ca^{2+} mobilization in FPR1- and FPR2-HL60 cells are reported in Tables 1 and 2. Considering the four stereoisomers of **6** it is evident that all of the compounds behaved as FPR1 antagonists, albeit with different potency, and that the absolute configuration of both chiral centers seems to be crucial for the interaction with FPR1. In fact, replacement of the (*S*)-tryptophan with (*R*)-tryptophan led to a 36-fold decrease in antagonist potency [(2*R*,2'*S*)-**6**: IC_{50} = 0.45 μM vs (2*R*,2'*R*)-**6**: IC_{50} = 16.5 μM], whereas exchange of (*R*)-phenylalanine with (*S*)- phenylalanine led to a less marked variation in potency [(2*R*,2'*S*)-**6**: IC_{50} = 0.45 μM vs (2*S*,2'*S*)-**6** IC_{50} = 5.8 μM]. In addition, (2*S*,2'*S*)-**6** was also able to block FPR2.

We next explored structural modifications on both ends of (2*R*,2'*S*)-**6** with the aim of understanding the structural requirements for optimal interaction with FPR1. First, we replaced the phenyl ring of the N-benzoyl moiety with substituents characterized by different volumes. This structural modification was inspired by previously reported data, which showed that the introduction of branched alkyl residues (i.e., *iso*-butyloxycarbonyl, *t*-butyloxycarbonyl, benzyloxycarbonyl) on the *N*-terminus of the peptide Met-Leu-Phe (MLF) resulted in antagonist activity, whereas the introduction of linear alkyl substituents (i.e., methoxycarbonyl, ethoxycarbonyl, and *n*-butyloxycarbonyl) resulted in agonist activity.[28,29] As an example, when the formyl group of the potent FPR1 agonist *f*MLF was replaced by a *t*-butyloxycarbonyl residue, the potent FPR1 antagonist Boc-MLF was obtained. On the basis of such considerations, we replaced the phenyl ring of the *N*-benzoyl group with cyclohexyl, isobutyl, and *t*-butoxy residues (Table 2). The activity data showed that the new derivatives behaved as FPR1 antagonists albeit the structural modifications differently affected antagonist potency. In fact, compound **10**, containing the cyclohexyl group, had an IC_{50} value comparable to that of (2*R*,2'*S*)-**6**. In contrast, introduction of the isobutyl (compound

11) or the *t*-butoxy substituents (compound (2*R*,2'*S*)-**8**) led to a marked reduction in antagonist potency. This effect was more pronounced for compound **11**, where a 43-fold decrease of potency was observed. These data indicate that the volume of the branched alkyl substituents plays a role in the interaction with FPR1. Moreover, introduction of the *t*-butoxy residue negatively affected selectivity of the compounds because compound (2*R*,2'*S*)-**8** was also able to activate FPR2. Finally, considering that compound (2*R*,2'*S*)-**7**, in which the phenylalanine moiety was replaced with cyclohexylalanine, had an IC_{50} value comparable to that of compound (2*R*,2'*S*)-**6**, we replaced the phenylalanine scaffold of (2*R*,2'*S*)-**6** with a branched amino acid, such as leucine or valine (compounds **12** and **13**, respectively). These structural modifications were not tolerated, because compounds **12** and **13** displayed a marked decrease in potency compared to both compounds (2*R*,2'*S*)-**6** (55- and 37-fold, respectively) and (2*R*,2'*S*)-**7** (26- and 17-fold, respectively). These data also suggest that for this part of the molecule, the shape and the size of the substituent is important for optimal interaction with FPR1. In addition, compound **12** was also able to activate FPR2. Subsequently, all compounds were further characterized in human neutrophils. We found that the compounds behaved as FPR1 antagonists, as they did not induce Ca^{2+} mobilization by themselves, but they dose-dependently blocked the response evoked by the potent agonist *f*MLF with IC_{50} values comparable to those observed in FPR1-HL60 cells, with the sole exception of compound **10** which had considerably lower antagonist potency in human neutrophils as compared to FPR1-HL60 cells.

Finally, since activation of neutrophils by *f*MLF can induce several functional responses including chemotaxis, we further investigated the effects of our most potent FPR1 antagonists (2*R*,2'*S*)-**6**, (2*R*,2'*S*)-**7**, (2*S*,2'*S*)-**6**, and **10** on neutrophil chemotaxis (Table 3). We found that all compounds dose-dependently inhibited *f*MLF-induced neutrophil migration. In addition, the observed IC_{50} values were in agreement with the antagonist potencies of the compounds. In particular, compounds (2*R*,2'*S*)-**6** and (2*R*,2'*S*)-**7** were confirmed to be highly potent FPR1 antagonists. On the other hand,

compound **10** had lower potency in chemotaxis inhibition than (2*R*,2'*S*)-**6** despite comparable antagonist potency on Ca^{2+} mobilization.

Conclusions

Starting from a dipeptide scaffold that is structurally related to the natural product aurantiamide, we have extended the structure-activity relationships of compounds (2*R*,2'*S*)-**6** and (2*R*,2'*S*)-**7**, which were reported as FPR1 antagonists. We have found that the absolute configuration *2R,2'S* is preferred to obtain potent FPR1 antagonists. The structural modifications performed on the terminal fragments of the molecule suggest that the size of the substituents can greatly influence the interaction with FPR1. All compounds behaved as antagonists in human neutrophils, and the most potent antagonists also inhibited chemotaxis. Considering that FPR1 is a key regulator of the inflammatory environment, the dipeptide derivatives described in this work may represent important leads for the development of new potent and selective FPR1 antagonists for the treatment of neutrophil-mediated inflammatory diseases.

Experimental Section

Chemistry. Chemicals were purchased from Sigma-Aldrich, Alfa Aesar, TCI Chemicals. Unless otherwise stated, all chemicals were used without further purification. Thin layer chromatography (TLC) was performed using plates from Merck (silica gel 60 F254). Column chromatography was performed with 1:30 Merck silica gel 60 Å (63-200 μm) as the stationary phase. Flash chromatographic separations were performed on a Biotage SP1 purification system using flash cartridges pre-packed with KP-Sil 32−63 μ m, 60 Å silica. Melting points were determined in open capillary on a Stuart electrothermal apparatus and were not corrected. ^{1}H NMR spectra were recorded on a Varian Mercury-VX spectrometer (300 MHz) or on a 500-vnmrs500 Agilent spectrometer (500 MHz). All chemical shift values are reported in ppm (δ). High resolution mass spectra (electrospray ionisation, ESI-TOF) (HRMS) were recorded on an Agilent 6530 Accurate

Mass Q-TOF (mass range 50-3000 *m/z*, dry gas nitrogen 10 mL/min, dry heater 325 °C, capillary voltage 4000 V, electrospray ion source in positive or negative ion mode). All spectra were in accordance with the assigned structures. Elemental analyses (C,H,N) of the target compounds were performed on a Eurovector Euro EA 3000 analyzer. Analyses indicated by the symbols of the elements were within ± 0.4 % of the theoretical values. The purity of the target compounds (Tables 1 and 2) was assessed by RP-HPLC and combustion analysis. All compounds showed ≥ 95% purity. RP-HPLC analysis was performed on an Agilent 1260 Infinity Binary LC System equipped with a diode array detector using a Phenomenex Luna C-8 column (250 x 4.6 mm, 5 μm particle size). All target compounds were eluted with MeOH/H_2O, 8:2 (v/v) at a flow rate of 1 mL/min. Enantiomeric purity of the target compounds was assessed by chiral HPLC analysis on a Perkin-Elmer series 200 LC instrument using a Daicel ChiralCell OD column (250 mm × 4.6 mm, 5 μm particle size) and equipped with a Perkin-Elmer 785A UV/VIS detector setting λ= 230 nm. The compounds were eluted with n-hexane/EtOH, 4:1, v/v at a flow rate of 0.8 mL/min. All compounds showed enantiomeric excesses (e.e.) >95%.

General Procedure for the Preparation of the Four Stereoisomers of compound 8 and compound 14.

N',N-Carbonyldiimidazole (0.14 g, 0.89 mmol) was added to a solution of (*R*)- or (*S*)-Boc-tryptophan (0.25 g, 0.81 mmol) in anhydrous THF (10 mL), and the reaction mixture was stirred overnight at room temperature. Next, a solution of the appropriate amino acid methyl ester in anhydrous THF (10 mL) was added and the reaction mixture was stirred for 24 h. The solvent was concentrated *in vacuo*, and the residue was dissolved in ethyl acetate (20 mL), washed first with saturated aqueous $NaHCO_3$, and then with 3 N HCl. The separated organic layer was dried over Na_2SO_4 and concentrated under reduced pressure. The crude residue was purified by flash chromatography as detailed below to give pure target compound.

(2*R*)-Methyl 2-[(2'*S*)-[(*tert*-butoxycarbonyl)amino]-3-(1*H*-indol-3-yl)propanamido]-3-phenylpropanoate (2*R*, 2'*S*-8). (Gradient elution from *n*-hexane/EtOAc, 7:3 to *n*-hexane/EtOAc, 3:7. White solid. 45% Yield). Melting point: 159-161 °C (from MeOH). ^{1}H NMR ($CDCl_3$): δ 1.40 (s, 9H, C(CH_3)$_3$), 2.79-2.81 (m, 1H, C*H*H-phenyl), 2.95 (dd, 1H, J_1= 5.4 Hz, J_2= 8.0 Hz, C*H*H-phenyl), 3.15 (dd, 1H, J_1= 7.6 Hz, J_2= 14.1 Hz, CH*H*-indolyl), 3.24-3.26 (m, 1H, CH*H*-indolyl), 3.60 (s, 3H, OCH_3), 4.45 (br s, 1H, NHC*H*$COCH_3$), 4.75-4.79 (m, 1H, NHC*H*CO), 5.07 (br s, 1H, N*H*CO), 6.24 (d, 1H, *J*= 7.8 Hz, OCON*H*), 6.80 (br d, 2H, ArH), 6.95 (s, 1H, ArH), 7.11-7.21 (m, 5H, ArH), 7.35 (d, 1H, *J*= 7.8 Hz, ArH), 7.64 (d, 1H, *J*= 7.8 Hz, ArH), 8.09 (s, 1H, N*H*). HRMS (ESI$^-$) calcd for [($C_{26}H_{31}N_3O_5$)-H]$^-$: 464.2191, found: 464.2176.

(2*S*)-Methyl 2-[(2'*R*)-[(*tert*-butoxycarbonyl)amino]-3-(1*H*-indol-3-yl)propanamido]-3-phenylpropanoate (2*S*, 2'*R*-8). (Gradient elution from *n*-hexane/EtOAc, 8:2 to *n*-hexane/EtOAc, 1:1. Yellow oil. 60% Yield). ^{1}H NMR ($CDCl_3$): δ 1.40 (s, 9H, C(CH_3)$_3$), 2.77-2.79 (m, 1H, C*H*H-phenyl), 2.94 (dd, 1H, J_1= 5.3 Hz, J_2= 8.0 Hz, C*H*H-phenyl), 3.16 (dd, 1H, J_1= 6.0 Hz, J_2= 7.8 Hz, CH*H*-indolyl), 3.26-3.28 (m, 1H, CH*H*-indolyl), 3.61 (s, 3H, OCH_3), 4.45 (br s, 1H, NHC*H*$COCH_3$), 4.77-4.78 (m, 1H, NHC*H*CO), 5.07 (br s, 1H, N*H*CO), 6.22 (br d, 1H, OCONH), 6.80 (br d, 2H, ArH), 6.95 (s, 1H, ArH), 7.12-7.21 (m, 5H, ArH), 7.35 (d, 1H, *J*= 7.8 Hz, ArH), 7.65 (d, 1H, *J*= 7.8 Hz, ArH), 8.05 (s, 1H, N*H*). HRMS (ESI$^-$) calcd for [($C_{26}H_{31}N_3O_5$)-H]$^-$: 464.2191, found: 464.2176.

(2*S*)-Methyl 2-[(2'*S*)-[(*tert*-butoxycarbonyl)amino]-3-(1*H*-indol-3-yl)propanamido])-3-phenylpropanoate (2*S*,2'*S*-8). (Gradient elution from *n*-hexane/EtOAc, 8:2 to *n*-hexane/EtOAc, 1:1. White solid. 41% Yield). Melting point: 153-155 °C (from MeOH). ^{1}H NMR ($CDCl_3$): δ 1.41 (s, 9H, C(CH_3)$_3$), 2.93 (d, 2H, *J*= 5.9 Hz, CH_2-phenyl), 3.13 (dd, 1H, J_1= 6.8 Hz, J_2= 7.3 Hz, CH*H*-indolyl), 3.27-3.29 (m, 1H, CH*H*-indolyl), 3.61 (s, 3H, OCH_3), 4.40-4.42 (m, 1H, NHC*H*$COCH_3$), 4.72-4.73 (m, 1H, NHC*H*CO), 5.11 (br s, 1H, N*H*CO), 6.21 (br s, 1H, OCON*H*), 6.80 (d, 2H, *J*=

6.8 Hz, ArH), 7.02 (s, 1H, ArH), 7.11-7.21 (m, 5H, ArH), 7.35 (d, 1H, *J*= 8.3 Hz, ArH), 7.65 (d, 1H, *J*= 7.8 Hz, ArH), 8.06 (s, 1H, N*H*). HRMS calcd for $C_{26}H_{31}N_3O_5$ (ES^-): 464.2191, found: 464.2188.

(2*R*)-Methyl 2-[(2'*R*)-[(*tert*-butoxycarbonyl)amino]-3-(1*H*-indol-3-yl)propanamido]-3-phenylpropanoate (2*R*,2'*R*-8). (Gradient elution from *n*-hexane/EtOAc, 8:2 to *n*-hexane/EtOAc, 1:1. Transparent oil. 75% Yield). ^{1}H NMR ($CDCl_3$): δ 1.41 (s, 9H, C(C*H*$_3$)$_3$), 2.93 (d, 2H, *J*= 5.9 Hz, C*H*$_2$-phenyl), 3.12 (dd, 1H, J_1= 6.8 Hz, J_2= 7.3 Hz, CH*H*-indolyl), 3.30-3.32 (m, 1H, CH*H*-indolyl), 3.61 (s, 3H, OCH_3), 4.41-4.43 (m, 1H, NHC*H*$COCH_3$), 4.70-4.72 (m, 1H, NHC*H*CO), 5.11 (br s, 1H, N*H*CO), 6.21 (br s, 1H, OCON*H*), 6.80 (d, 2H, *J*= 6.8 Hz, ArH), 7.0 (br s, 1H, ArH), 7.11-7.25 (m, 5H, ArH), 7.35 (d, 1H, *J*= 8.3 Hz, ArH), 7.65 (d, 1H, *J*= 7.8 Hz, ArH), 8.06 (s, 1H, N*H*). HRMS (ESI^-) calcd for [($C_{26}H_{31}N_3O_5$)-H]$^-$: 464.2191, found: 464.2176.

(2*R*)-Methyl 2-[(2'*S*)-[(*tert*-butoxycarbonyl)amino]-3-(1*H*-indol-3-yl)propanamido]-4-methylpentanoate (14). (Gradient elution from *n*-hexane/EtOAc, 7:3 to *n*-hexane/EtOAc, 3:7. Yellow oil. 41% Yield). ^{1}H NMR ($CDCl_3$): δ 0.97 (d, 6H, *J*= 5.8 Hz, CH(C*H*$_3$)$_2$), 1.41 (s, 9H, C(C*H*$_3$)$_3$), 1.45-1.48 (m, 1H, C*H*$(CH_3)_2$), 1.87-1.93 (m, 2H, C*H*$_2$CH$(CH_3)_2$), 3.10 (dd, 1H, J_1= 6.8 Hz, J_2= 7.3 Hz, CH*H*-indolyl), 3.30-3.32 (m, 1H, C*H*H-indolyl), 3.63 (s, 3H, OCH_3), 4.45-4.48 (m, 2H, NHC*H*$COCH_3$, NHC*H*CO), 5.11 (br s, 1H, N*H*CHCO), 6.17 (br d, 1H, OCON*H*), 7.07 (s, 1H, ArH), 7.12 (t, 1H, *J*= 7.3 Hz, ArH), 7.19 (t, 1H, *J*= 7.3 Hz, ArH), 7.35 (d, 1H, *J*= 7.8 Hz, ArH), 7.65 (d, 1H, *J*= 7.8 Hz, ArH), 8.16 (s, 1H, N*H*). HRMS (ESI^-) calcd for [($C_{23}H_{33}N_3O_5$)-H]$^-$: 430.2347, found: 430.2338.

(2*R*)-Methyl 2-[(2'*S*)-[(*tert*-butoxycarbonyl)amino]-3-(1*H*-indol-3-yl)propanamido]-3-methylbutanoate (15).

A solution of Boc-(*S*)-tryptophan (0.20 g, 0.66 mmol), (*R*)-valine methyl ester (0.10 g, 0.79 mmol), PyBOP (0.53 g, 0.98 mmol), and *N*-methylmorpholine (0.50 mL, 5.2 mmol) in anhydrous DMF (10 mL) was stirred overnight at room temperature. H_2O was added, and the reaction mixture was extracted with AcOEt (3 × 20mL). The combined organic layers were washed with brine, dried over Na_2SO_4, and concentrated *in vacuo*. The crude residue was chromatographed by silica gel chromatography using $CHCl_3$/EtOAc 1:1 as eluent to obtain the pure compound as colorless oil (0.21 g, 77% yield). ^{1}H NMR ($CDCl_3$): δ 0.69 (d, 3H, *J*= 6.4 Hz, CH(C*H*$_3$)$_2$), 0.75 (d, 3H, *J*= 6.4 Hz, CH(C*H*$_3$)$_2$), 1.41 (s, 9H, C(C*H*$_3$)$_3$), 2.01-2.04 (m, 1H, C*H*(CH$_3$)$_2$), 3.20 (dd, 1H, J_1= 7.0 Hz, J_2= 14.6 Hz, CH*H*-indolyl), 3.31 (dd, 1H, J_1= 6.4 Hz, J_2= 14.0 Hz, C*H*H-indolyl), 3.63 (s, 3H, OCH$_3$), 4.42-4.46 (m, 1H, NHC*H*COCH$_3$), 4.50 (br s, 1H, NHC*H*CO), 5.07 (br s, 1H, N*H*CHCO), 6.34 (br d, 1H, OCON*H*), 7.07 (s, 1H, ArH), 7.11 (t, 1H, *J*= 7.1 Hz, ArH), 7.19 (t, 1H, *J*= 7.2 Hz, ArH), 7.34 (d, 1H, *J*= 8.2 Hz, ArH), 7.63 (d, 1H, *J*= 7.6 Hz, ArH), 8.15 (s, 1H, N*H*). HRMS (ESI$^-$) calcd for [($C_{22}H_{31}N_3O_5$)-H]$^-$: 417.2264, found: 417.2186.

General Procedure for the Preparation of the Four Stereoisomers of compound 9, and compounds 16-17.

Trifluoroacetic acid (0.85 mL) was added to a solution of Boc-protected derivative **8, 14, 15** (0.33 mmol) in CH_2Cl_2 (10 mL). The reaction mixture was stirred at room temperature for 5 h and alkalinized with aqueous 5% NaOH. The separated aqueous phase was extracted with CH_2Cl_2 (3 × 20mL). The combined organic layers were dried (Na_2SO_4) and concentrated under reduced pressure to obtain the desired compound, which was used without further purification.

(2*R*)-Methyl 2-[(2'*S*)-amino-3-(1*H*-indol-3-yl)propanamido]-3-phenylpropanoate (2*R*,2'*S*-9). (Colorless oil, quantitative yield.) ^{1}H NMR ($CDCl_3$): δ 1.78 (br s, 2H, NH_2, D_2O exchanged), 2.82-2.83 (m, 1H, C*H*H-phenyl), 2.95 (dd, 1H, J_1= 5.4 Hz, J_2= 8.0 Hz, C*H*H-phenyl), 3.15 (dd, 1H, J_1= 7.6 Hz, J_2= 14.1 Hz, CH*H*-indolyl), 3.24-3.26 (m, 1H, CH*H*-indolyl), 3.60 (s, 3H, OCH$_3$), 4.45 (br

s, 1H, NHC*H*COCH$_3$), 4.75-4.79 (m, 1H, NHC*H*CO), 6.24 (d, 1H, *J*= 7.8 Hz, ArH), 6.80 (br d, 2H, ArH), 6.95 (br s, 1H, N*H*CO), 7.11-7.21 (m, 5H, ArH), 7.35 (d, 1H, *J*= 7.8 Hz, ArH), 7.64 (d, 1H, *J*= 7.8 Hz, ArH), 8.09 (s, 1H, N*H*). HRMS (ESI$^+$) calcd for [($C_{21}H_{23}N_3O_3$)+H]$^+$: 366.1812, found: 366.1818.

(2*S*)-Methyl 2-[(2'*R*)-amino-3-(1*H*-indol-3-yl)propanamido]-3-phenylpropanoate (2*S*,2'*R*-9). (Colorless oil, 83% yield). ^{1}H NMR ($CDCl_3$): δ 1.82 (br s, 2H, NH_2, D_2O exchanged), 2.84-2.89 (m, 1H, C*H*H-phenyl), 2.95 (dd, 1H, J_1= 5.4 Hz, J_2= 8.0 Hz, C*H*H-phenyl), 3.16 (dd, 1H, J_1= 6.0 Hz, J_2= 7.8 Hz, CH*H*-indolyl), 3.23-3.25 (m, 1H, CH*H*-indolyl), 3.63 (s, 3H, OCH_3), 4.45 (br s, 1H, NHC*H*COCH$_3$), 4.75-4.79 (m, 1H, NHC*H*CO), 6.24 (d, 1H, *J*= 7.8 Hz, ArH), 6.80 (br d, 2H, ArH), 6.95 (br s, 1H, N*H*CO), 7.11-7.21 (m, 5H, ArH), 7.35 (d, 1H, *J*= 7.8 Hz, ArH), 7.64 (d, 1H, *J*= 7.8 Hz, ArH), 8.09 (s, 1H, N*H*). HRMS (ESI$^+$) calcd for [($C_{21}H_{23}N_3O_3$)+H]$^+$: 366.1812, found: 366.1809.

(2*S*)-methyl 2-[(2'*S*)-amino-3-(1*H*-indol-3-yl)propanamido]-3-phenylpropanoate (2*S*,2'*S*-9). (Yellow oil, 95% yield). ^{1}H NMR ($CDCl_3$): δ 1.80 (br s, 2H, NH_2, D_2O exchanged), 2.89 (dd, 1H, J_1= 8.3 Hz, J_2= 14.7 Hz, CH*H*-indolyl), 3.02-3.04 (m, 2H, CH_2-phenyl), 3.20 (dd, 1H, J_1= 4.4 Hz, J_2= 14.7 Hz, C*H*H-indolyl), 3.63 (s, 3H, OCH_3), 3.70-3.74 (m, 1H, NHC*H*COCH$_3$), 4.87 (q, 1H, *J*= 6.4 Hz, NHC*H*CO), 6.94-6.96 (m, 2H, ArH), 7.01 (s, 1H, CON*H*), 7.13 (t, 1H, *J*= 7.8 Hz, ArH), 7.17-7.21 (m, 4H, ArH), 7.36 (d, 1H, *J*= 8.3 Hz, ArH), 7.66 (d, 1H, *J*= 5.9 Hz, ArH), 7.72 (d, 1H, *J*= 8.3 Hz, ArH), 8.15 (s, 1H, N*H*). HRMS (ESI$^+$) calcd for [($C_{21}H_{23}N_3O_3$)+H]$^+$: 366.1812, found: 366.1812.

(2*R*)-Methyl 2-[(2'*R*)-amino-3-(1*H*-indol-3-yl)propanamido]-3-phenylpropanoate (2*R*,2'*R*-9). (Colorless oil, 83% yield). ^{1}H NMR ($CDCl_3$): δ 1.80 (br s, 2H, NH_2, D_2O exchanged), 2.89 (dd, 1H, J_1= 8.3 Hz, J_2= 14.7 Hz, CH*H*-indolyl), 3.02-3.04 (m, 2H, CH_2-phenyl), 3.25 (dd, 1H, J_1= 4.4 Hz,

J_2= 14.7 Hz, CH*H*-indolyl), 3.69 (s, 3H, OCH_3), 3.70-3.74 (m, 1H, NHC*H*$COCH_3$), 4.87 (q, 1H, *J*= 6.4 Hz, NHC*H*CO), 6.94-6.96 (m, 2H, ArH), 7.01 (s, 1H, CON*H*), 7.13 (t, 1H, *J*= 7.8 Hz, ArH), 7.17-7.21 (m, 4H, ArH), 7.36 (d, 1H, *J*= 8.3 Hz, ArH), 7.66 (d, 1H, *J*= 5.9 Hz, ArH), 7.72 (d, 1H, *J*= 8.3 Hz, ArH), 8.15 (s, 1H, N*H*). HRMS (ESI^+) calcd for $[(C_{21}H_{23}N_3O_3)+H]^+$: 366.1812, found: 366.1812.

(2*R*)-Methyl 2-[(2'*S*)-amino-3-(1*H*-indol-3-yl)propanamido]-4-methylpentanoate (16). (Colorless oil. 76% Yield). ^1H NMR ($CDCl_3$): δ 0.97 (d, 6H, *J*= 5.9 Hz, $CH(CH_3)_2$), 1.54-1.65 (m, 3H, $CH_2CH(CH_3)_2$), 2.02-2.04 (br s, 2H, NH_2, D_2O exchanged), 2.95 (dd, 1H, J_1= 8.8 Hz, J_2= 14.6 Hz, CH*H*-indolyl), 3.39 (dd, 1H, J_1= 4.1 Hz, J_2= 14.6 Hz, C*H*H-indolyl), 3.70 (s, 3H, OCH_3), 3.81 (q, 1H, *J*= 4.7 Hz, NHC*H*$COCH_3$), 4.57-4.59 (m, 1H, NHC*H*CO), 7.11-7.22 (m, 3H, ArH, N*H*CO), 7.36 (d, 1H, *J*= 8.2 Hz, ArH), 7.65-7.68 (d, 2H, *J*= 7.6 Hz, ArH), 8.21 (s, 1H, N*H*). HRMS (ESI^+) calcd for $[(C_{18}H_{25}N_3O_3)+H]^+$: 332.1969, found: 332.1972.

(2*R*)-Methyl 2-[(2'*S*)-amino-3-(1*H*-indol-3-yl)propanamido]-3-methylbutanoate (17). (Yellow oil. 61% Yield). ^1H NMR ($CDCl_3$): δ 0.92-0.99 (m, 6H, $CH(CH_3)_2$), 2.24-2.39 (m, 3H, $CH(CH_3)_2$, NH_2, 2H D_2O exchanged), 3.08 (dd, 1H, J_1= 7.0 Hz, J_2= 14.6 Hz, CH*H*-indolyl), 3.28 (dd, 1H, J_1= 4.4 Hz, J_2= 14.6 Hz, C*H*H-indolyl), 3.68 (s, 3H, OCH_3), 3.84-4.00 (m, 1H, NHC*H*$COCH_3$), 4.30-4.55 (m, 1H, NHC*H*CO), 6.99-7.23 (m, 3H, ArH, N*H*CO), 7.42 (d, 1H, *J*= 7.2 Hz, ArH), 7.72 (d, 1H, *J*= 7.2 Hz, ArH), 7.83 (d, 1H, *J*= 7.6 Hz, ArH), 8.21 (s, 1H, N*H*). HRMS (ESI^+) calcd for $[(C_{17}H_{23}N_3O_3)+H]^+$: 318.1812, found: 366.1812.

General Procedure for the Preparation of the Four Stereoisomers of Compound 6 and compounds 10-13.

N'N-Carbonyldiimidazole (0.05 g, 0.33 mmol) was added to a solution of the appropriate carboxylic acid (0.31 mmol) in anhydrous THF (10 mL) under N_2. The reaction mixture was stirred

at room temperature overnight. A solution of the appropriate amine in anhydrous THF (10 mL) was added, and the reaction mixture was stirred at room temperature for 24 h. The solvent was removed *in vacuo*, and the residue was partitioned between EtOAc (20 mL) and H_2O (2 × 20 mL). The aqueous layer was separated and extracted twice with EtOAc (20 mL). The collected organic layers were washed with saturated aqueous $NaHCO_3$, dried over Na_2SO_4 and concentrated under reduced pressure. The crude residue was purified by column chromatography as detailed below to obtain pure target compounds.

(2*R*)-Methyl 2-[(2'*S*)-2-benzamido-3-(1*H*-indol-3-yl)propanamido]-3-phenylpropanoate (2*R*,2'*S*-6). (Eluted with $CHCl_3$/EtOAc, 8:2. Pale yellow solid. 50% yield). Melting point: 170-172 °C (from MeOH). ^{1}H NMR ($CDCl_3$): δ 2.80 (dd, 1H, *J* = 5.9 and 13.7 Hz, C*H*H-phenyl), 2.95 (dd, 1H, *J* = 5.9 and 13.7 Hz, C*H*H-phenyl), 3.23 (dd, 1H, *J* = 8.3 and 14.2 Hz, CH*H*-indolyl), 3.44 (dd, 1H, *J* = 5.4 and 14.7 Hz, CH*H*-indolyl), 3.63 (s, 3 H, OCH_3), 4.79 (app q, 1H, NHC*H*$COCH_3$), 4.95 (app q, 1H, NHC*H*CO), 6.21 (br d, 1H, amide), 6.80 (d, 2H, *J* = 7.3 Hz, ArH), 6.88-6.91 (m, 2H, ArH, PhCON*H*), 7.12 (app t, 2H, ArH), 7.17 (app t, 2H, ArH), 7.24 (app t, 1H, ArH), 7.37-7.42 (m, 3H, ArH), 7.50 (app t, 1H, ArH), 7.70 (d, 2H, *J* = 7.8 Hz, ArH), 7.79 (d, 1H, *J* = 7.8 Hz, ArH), 8.07 (s, 1H, N*H*). HRMS (ESI$^-$) calcd for [($C_{28}H_{27}N_3O_4$)-H]$^-$: 468.1929, found: 468.1925.

(2*S*)-Methyl 2-[(2'*R*)-benzamido-3-(1*H*-indol-3-yl)propanamido]-3-phenylpropanoate (2*S*,2'*R*-6). (Gradient elution from *n*-hexane/EtOAc, 7:3 to *n*-hexane/EtOAc 2:8. White solid. 23% Yield). Melting point: 140-142 °C (from MeOH). ^{1}H NMR ($CDCl_3$): δ 2.78 (dd, 1H, J_1= 5.4 Hz, J_2= 13.7 Hz, C*H*H-phenyl), 2.94 (dd, 1H, J_1= 5.9, Hz, J_2= 14.2 Hz, CH*H*-phenyl), 3.21 (dd, 1H, J_1= 8.3 Hz, J_2= 14.7 Hz, C*H*H-indolyl), 3.42 (dd, 1H, J_1= 4.9 Hz, J_2= 14.2 Hz, CH*H*-indolyl), 3.61 (s, 3H, OCH_3), 4.76-4.80 (m, 1H, NHC*H*$COCH_3$), 4.92-4.96 (m, 1H, NHC*H*CO), 6.20 (d, 1H, *J*=7.8 Hz, amide), 6.78 (d, 2H, *J*=8.3 Hz, ArH), 6.88-6.89 (m, 2H, ArH, PhCON*H*), 6.90-7.12 (m, 2H, ArH), 7.14-7.18 (m, 2H, ArH), 7.22 (td, 1H, J_1= 1.8 Hz, J_2= 7.3 Hz, ArH), 7.36-7.41 (m, 3H,

ArH), 7.47-7.50 (m, 1H, ArH), 7.68-7.70 (m, 2H, ArH), 7.77 (d, 1H, *J*=7.82 Hz, ArH), 8.07 (s, 1H, N*H*). HRMS (ESI$^-$) calcd for [($C_{28}H_{27}N_3O_4$)-H]$^-$: 468.1929, found: 468.1924.

(2*S*)-Methyl 2-[(2'*S*)-benzamido-3-(1*H*-indol-3-yl)propanamido]-3-phenylpropanoate (2*S*,2'*S*-6). (Eluted with $CHCl_3$/EtOAc, 8:2. Yellow solid. 50% Yield). Melting point: 173-175 °C (from MeOH). ^{1}H NMR ($CDCl_3$): δ 2.02 (dd, 1H, J_1= 6.4 Hz, J_2= 14.2 Hz, C*H*H-phenyl), 3.02 (dd, 1H, J_1= 4.9 Hz, J_2= 14.2 Hz, C*H*H-indolyl), 3.18 (dd, 1H, J_1= 8.3 Hz, J_2= 14.7 Hz, CH*H*-phenyl), 3.49 (dd, 1H, J_1= 4.9 Hz, J_2= 14.7 Hz, CH*H*-indolyl), 3.68 (s, 3H, OCH_3), 4.71 (app q, 1H, NHC*H*$COCH_3$), 4.88-4.95 (m, 1H, NHC*H*CO), 6.12 (br d, 1H, amide), 6.87 (d, 2H, *J*= 7.3 Hz, ArH), 6.95 (br d, 1H, PhCON*H*), 7.04-7.08 (m, 2H, ArH), 7.10-7.16 (m, 3H, ArH), 7.22 (app t, 1H, ArH), 7.33-7.42 (m, 3H, ArH), 7.48-7.52 (m, 1H, ArH), 7.69 (app d, 2H, ArH), 7.79 (d, 1H, *J*= 7.8 Hz, ArH), 8.06 (s, 1H, N*H*). HRMS (ESI$^-$) calcd for [($C_{28}H_{27}N_3O_4$)-H]$^-$: 468.1929, found: 468.1924.

(2*R*)-Methyl 2-[(2'*R*)-benzamido-3-(1*H*-indol-3-yl)propanamido]-3-phenylpropanoate (2*R*,2'*R*-6). (Eluted with $CHCl_3$/EtOAc, 8:2. Transparent oil. 30% Yield). Melting point: 142-144 °C (from MeOH). ^{1}H NMR ($CDCl_3$): δ 2.90 (dd, 1H, J_1= 6.4 Hz, J_2= 13.7 Hz, C*H*H-phenyl), 2.99 (dd, 1H, J_1= 5.4 Hz, J_2= 13.7 Hz, CH*H*-phenyl), 3.19 (dd, 1H, J_1= 8.3 Hz, J_2= 14.7 Hz, C*H*H-indolyl), 3.48 (dd, 1H, J_1= 4.9 Hz, J_2= 14.7 Hz, CH*H*-indolyl), 3.65 (s, 3H, OCH_3), 4.70 (app q, 1H, NHC*H*$COCH_3$), 4.90-4.93 (m, 1H, NHC*H*CO), 6.16 (d, 1H, *J*= 6.8 Hz, amide), 6.81 (d, 2H, *J*= 7.3 Hz, ArH), 6.95 (d, 1H, *J*= 6.85 Hz, PhCON*H*), 7.06 (app t, 3H, ArH), 7.10-7.15 (m, 3H, ArH), 7.22 (t, 1H, *J*= 7.3 Hz, ArH), 7.36-7.42 (m, 3H, ArH), 7.50 (t, 1H, *J*= 7.3 Hz, ArH), 7.70 (d, 1H, *J*=7.83 Hz, ArH), 7.78 (d, 1H, *J*= 7.8 Hz, ArH), 8.07 (s, 1H, N*H*). HRMS (ESI$^-$) calcd for [($C_{28}H_{27}N_3O_4$)-H]$^-$: 468.1929, found: 468.1925.

(2*R*)-Methyl 2-[(2'*S*)-2-cyclohexanecarboxamido-3-(1*H*-indol-3-yl)propanamido]-3-phenylpropanoate (10). (Eluted with $CHCl_3$/EtOAc, 1:1. White solid. 20% yield). Melting point:

195-196 °C (from MeOH). ^{1}H NMR ($CDCl_3$): δ 1.17-1.27 (m, 3H, cyclohexane), 1.33-1.47 (m, 2H, cyclohexane), 1.62-1.66 (m, 2H, cyclohexane), 1.72-1.77 (m, 3H, cyclohexane), 2.02 (app t, 1H, $(CH_2)_2CHCO$), 2.79 (dd, 1H, J_1= 5.4 Hz, J_2= 13.2 Hz, C*H*H-phenyl), 2.92 (dd, 1H, J_1= 5.4 Hz, J_2= 13.7 Hz, C*H*H-phenyl), 3.10 (dd, 1H, J_1= 5.9 Hz, J_2= 13.2 Hz, C*H*H-indolyl), 3.25-3.27 (m, 1H, CH*H*-indolyl), 3.62 (s, 3H, OCH_3), 4.75 (br s, 2H, NHC*H*$COCH_3$, NHC*H*CO), 6.15 (br s, 1H, amide), 6.23 (br s, 1H, cyclohexane-CON*H*), 6.81-6.85 (m, 3H, ArH), 7.13-7.22 (m, 4H, ArH), 7.35 (d, 2H, *J*= 7.8 Hz, ArH), 7.70 (d, 1H, *J*= 7.8 Hz, ArH), 8.08 (s, 1H, N*H*). HRMS (ESI$^-$) calcd for $[(C_{28}H_{33}N_3O_4)-H]^-$: 474.2398, found: 474.2392.

(2*R*)-Methyl 2-[(2'*S*)-3-(1*H*-indol-3-yl)-2-(3-methylbutanamido)propanamido]-3-phenylpropanoate (11). (Eluted with $CHCl_3$/EtOAc, 8:2. White solid. 15% Yield). Melting point: 181-182 °C (from MeOH). ^{1}H NMR ($CDCl_3$): δ 0.87 (d, 6H, *J*=5.8 Hz, $(CH_3)_2CH$), 1.99-2.14 (m, 3H, $(CH_3)_2CHCH_2$), 2.74 (dd, 1H, J_1= 5.9 Hz, J_2= 14.1 Hz, C*H*H-phenyl), 2.91 (dd, 1H, J_1= 5.9 Hz, J_2= 13.5 Hz, CH*H*-phenyl), 3.09 (dd, 1H, J_1= 8.2 Hz, J_2= 14.6 Hz, C*H*H-indolyl), 3.28 (dd, 1H, J_1= 5.3 Hz, J_2= 14.6 Hz, CH*H*-indolyl), 3.62 (s, 3H, OCH_3), 4.73-4.77 (m, 2H, NHC*H*$COCH_3$, NHC*H*CO), 6.12 (app t, 2H, amide, CH_2CON*H*), 6.77 (app d, 2H, ArH), 6.87 (br s, 1H, ArH), 7.13 (s, 1H, ArH), 7.13-7.22 (m, 4H, ArH), 7.36 (d, 1H, *J*= 7.6 Hz, ArH), 7.71 (d, 1H, *J*= 7.6 Hz, ArH), 8.05 (s, 1H, N*H*). HRMS (ESI$^-$) calcd for $[(C_{26}H_{31}N_3O_4)-H]^-$: 448.2242, found: 448.2237.

(2*R*)-Methyl 2-[(2'S)-2-benzamido-3-(1*H*-indol-3-yl)propanamido]-4-methylpentanoate (12). (Eluted with $CHCl_3$/EtOAc, 8:2. White solid. 17% Yield). Melting point: 89-91 °C (from MeOH). ^{1}H NMR ($CDCl_3$): δ 0.80 (d, 6H, *J*= 9.8 Hz, $(CH_3)_2CH$), 1.23-1.30 (m, 2H, $(CH_3)_2CHCH_2$), 1.35-1.41 (m, 1H, $(CH_3)_2CH$), 3.24 (dd, 1H, J_1= 8.0 Hz, J_2= 14.1 Hz, C*H*H-indolyl), 3.48 (dd, 1H, J_1= 4.7 Hz, J_2= 14.1 Hz, CH*H*-indolyl), 3.63 (s, 3H, OCH_3), 4.45-4.50 (m, 1H, NHC*H*$COCH_3$), 4.99-5.02 (m, 1H, NHC*H*CO), 6.09 (br s, 1H, amide), 6.94 (d, 1H, *J*=7.0 Hz, PhCON*H*), 7.13-7.22 (m, 3H, ArH), 7.36-7.42 (m, 3H, ArH), 7.47-7.49 (m, 1H, ArH), 7.70-7.73

(m, 2H, ArH), 7.76-7.78 (m, 1H, ArH), 8.13 (s, 1H, N*H*). HRMS (ESI$^-$) calcd for [($C_{25}H_{29}N_3O_4$)-H]$^-$: 434.2085, found: 434.2081.

(2*R*)-Methyl 2-[(2'*S*)-2-benzamido-3-(1*H*-indol-3-yl)propanamido]-3-methylbutanoate (13). (Eluted with $CHCl_3$/EtOAc, 8:2. White solid. 23% Yield). Melting point: 77-79 °C (from MeOH). ^{1}H NMR ($CDCl_3$): δ 0.65 (d, 3H, *J*= 7.0 Hz, C*H*$_3$CHCH$_3$), 0.71 (d, 3H, *J*= 7.0 Hz, CH$_3$CHC*H*$_3$), 1.93-1.97 (m, 1H, CH$_3$C*H*CH$_3$), 3.27 (dd, 1H, J_1= 7.0 Hz, J_2= 14.1 Hz, C*H*H-indolyl), 3.50 (dd, 1H, J_1= 4.1 Hz, J_2= 14.1 Hz, CH*H*-indolyl), 3.63 (s, 3H, OCH$_3$), 4.40 (app q, 1H, NHC*H*COCH$_3$), 5.03-5.06 (m, 1H, NHC*H*CO), 6.31 (br d, 1H, amide), 6.91-6.93 (m, 1H, PhCON*H*), 7.13-7.19 (m, 2H, ArH), 7.21 (app, t, 1H, ArH), 7.39 (app t, 3H, ArH), 7.46-7.51 (m, 1H, ArH), 7.70 (d, 2H, *J*= 7.6 Hz, ArH), 7.78 (d, 1H, *J*= 7.6 Hz, ArH), 8.17 (s, 1H, NH). HRMS (ESI$^-$) calcd for [($C_{24}H_{27}N_3O_4$)-H]$^-$: 420.1929, found: 420.1924.

Pharmacology

Cell culture. Human promyelocytic leukemia HL60 cells stably transfected with FPR1 (FPR1-HL60 cells) or FPR2 (FPR2-HL60 cells) were cultured in RPMI 1640 medium supplemented with 10% heat-inactivated fetal calf serum, 10 mM HEPES, 100 μg/ml streptomycin, 100 U/ml penicillin, and G418 (1 mg/mL). Although stable cell lines are cultured under G418 selection pressure, G418 may affect some assays, so it was removed in the last round of culture before assays were performed.

Isolation of human neutrophils. Blood was collected from healthy donors. All experiments were performed in accordance with the Guidelines of the Office of Human Research Protections, United States Department of Health and Human Services, and experiments were approved by the Institutional Review Board at Montana State University (Protocol # MQ041017). Informed consents were obtained from human participants of this study. Neutrophils were purified from the blood using dextran sedimentation, followed by Histopaque 1077 gradient separation and hypotonic

lysis of red blood cells. Isolated neutrophils were washed twice and resuspended in HBSS without Ca^{2+} and Mg^{2+} ($HBSS^-$). Neutrophil preparations were routinely >95 % pure, as determined by light microscopy, and > 98 % viable, as determined by trypan blue exclusion.

Ca^{2+} mobilization assay. Changes in intracellular Ca^{2+} were measured with a FlexStation II scanning fluorometer (Molecular Devices, Sunnyvale, CA, USA). The cells, suspended in $HBSS^-$ containing 10 mM HEPES, were loaded with Fluo-4 AM dye (1.25 μg/mL final concentration) and incubated for 30 min in the dark at 37 °C. After dye loading, the cells were washed with $HBSS^-$ containing 10 mM HEPES, resuspended in HBSS with Ca^{2+} and Mg^{2+} ($HBSS^+$). $HBSS^+$ containing 10 mM HEPES, and aliquoted into the wells of a flat-bottom, half-area-well black microtiter plates (2 x 10^5 cells/well). For evaluation of direct agonist activity, the compound of interest was added from a source plate containing dilutions of test compounds in $HBSS^+$, and changes in fluorescence were monitored (λ_{ex} = 485 nm, λ_{em} = 538 nm) every 5 s for 240 s at room temperature after automated addition of compounds.

Antagonist activity and selectivity were evaluated after a 30 min pretreatment with test compounds at room temperature, followed by addition of peptide agonist (5 nM *f*MLF for FPR1-HL60 cells and neutrophils or 5 nM WKYMVM for FPR2-HL60 cells). In some experiments, a range of *f*MLF concentrations was used. Maximum change in fluorescence during the first 3 min, expressed in arbitrary units over baseline, was used to determine a response. Responses for FPR1 antagonists were normalized to the response induced by 5 nM *f*MLF for FPR1-HL60 cells and neutrophils, or 5 nM WKYMVm for FPR2-HL60 cells, which were assigned a value of 100%. Curve fitting (5-6 points) and calculation of median effective inhibitory concentrations (IC_{50}) were performed by nonlinear regression analysis of the dose–response curves generated using Prism 7 (GraphPad Software, Inc., San Diego, CA, USA). Efficacy is expressed as % inhibition by an antagonist of the response induced by 5 nM *f*MLF at the maximal applied concentration of an antagonist (~ 50 μM).

Chemotaxis assay

Human neutrophils were resuspended in $HBSS^+$ containing 2% (v/v) heat-inactivated fetal bovine serum (FBS) (2×10^6 cells/ml), and chemotaxis was analyzed in 96-well ChemoTx chemotaxis chambers (Neuroprobe, Gaithersburg, MD, USA). Briefly, neutrophils were preincubated with the indicated concentrations of the tested compounds or dimethyl sulfoxide (DMSO) for 30 min at room temperature and added to the upper wells of the ChemoTx chemotaxis chambers. The lower wells were loaded with 30 µl of $HBSS^+$ containing 2% (v/v) heat-inactivated FBS with the indicated concentrations of test compounds plus 1 nM *f*MLF, DMSO plus 1 nM *f*MLF (positive control), or DMSO alone (negative control). Neutrophils were allowed to migrate through the 5.0-µm pore polycarbonate membrane filter for 60 min at 37 °C and 5% CO_2. The number of migrated cells was determined by measuring ATP in lysates of transmigrated cells using a luminescence-based assay (CellTiter-Glo; Promega, Madison, WI, USA) and a Fluoroscan Ascent FL microplate reader. Luminescence measurements were converted to absolute cell numbers by comparison of the values with standard curves obtained with known numbers of neutrophils. Curve fitting (at least eight to nine points) and calculation of median effective concentration values (IC_{50}) were performed by nonlinear regression analysis of the dose–response curves generated using Prism software.

Conflicts of interest

There are no conflicts to declare.

Acknowledgements

This research was supported in part by National Institutes of Health IDeA Program COBRE Grant GM110732; USDA National Institute of Food and Agriculture Hatch project 1009546; and the Montana State University Agricultural Experiment Station. We thank Marie-Josèphe Rabiet (INSERM, Grenoble, France) for the kind gift of FPR-transfected HL60 cells.

References

1. K. Cheng, Z. Bao, W. Gong, P. Tang, T. Yoshimura, J- M. Wang, Regulation of inflammation by members of the formyl-peptide receptor family, *J. Autoimm.,* 2017, **85**, 64.

2. R. D. Ye, F. Boulay, J. M. Wang, C. Dahlgren, C. Gerard, M. Parmentier, C. N. Serhan, P. M. Murphy, International Union of Basic and Clinical Pharmacology: LXXIII. Nomenclature for the formyl peptide receptor (FPR) family. *Pharmacol. Rev.*, 2009, **61**, 119.

3. H.Q. He, R. D. Ye, The formyl peptide receptors: diversity of ligands and mechanism for recognition, *Molecules*, 2017, **22**, 455.

4. E. Schiffmann, B.A. Corcoran, S.M. Wahl, N-formylmethionyl peptides as chemoattractants for leucocytes, *Proc. Natl. Acad. Sci. U.S.A.*, 1975, **72**, 1059.

5. Y. Le, J.J. Oppenheim, J.M. Wang, Pleiotropic roles of formyl peptide receptors, *Cytokine Growth Factor Rev.*, 2001, **12**, 91.

6. T. Y. Cheng, M. S. Wu, J. T. Lin, M. T. Lin, C. T. Shun, K. T. Hua, M. L. Kuo, Formyl Peptide receptor 1 expression is associated with tumor progression and survival in gastric cancer, *Anticancer Res.,* 2014, **34**, 2223.

7. L. Zhang, H. Wang, T. Yang, Z. Su, D. Fang, Y. Wang, J. Fang, X. Hou, Y. Le, K. Chen, J. M. Wang, S. B. Su, Q. Lin, Q. Zhou, Formylpeptide receptor 1 mediates the tumorigenicity of human hepatocellular carcinoma cells, *OncoImmunology*, 2016, **5**, e1078055.

8. J. Huang, K. Chen, J. Chen, W. Gong, N. M. Dunlop, O. M. Howard, Y. Gao, X. W. Bian, J. M. Wang, The G-protein-coupled formylpeptide receptor FPR confers a more invasive phenotype on human glioblastoma cells, *Br. J. Cancer*, 2010, **102**, 1052.

9. J. Huang, J. Hu, X. Bian, K. Chen, W. Gong, N. M. Dunlop, O. M. Howard, J. M. Wang, Transactivation of the epidermal growth factor receptor by for- mylpeptide receptor exacerbates the malignant behavior of human glio- blastoma cells, *Cancer Res.,* 2007, **67**, 5906.

10. I. Snapkov, C. O. Oqvist, Y. Figenschau, P. Kogner, J. I. Johnsen, B. Sveinbjornsson, The role of formyl peptide receptor 1 (FPR1) in neuroblastoma tumorigenesis, *BMC Cancer,* 2016, **16**, 490.

11. M. F. Salamah, D. Ravishankar, R. Vaiyapuri, L. A. Moraes, K. Patel, M. Perretti, J. M. Gibbins, S. Vaiyapuri, The formyl peptide fMLF primes platelet activation and augments thrombus formation, *J. Thromb. Haemost.,* 2019, **17**, 1120.

12. M. Honda, T. Takeichi, K. Asonuma, Y. Inomata, Intravital two-photon imaging of neutrophil recruitment reveals an efficacy of FPR1 blockade to attenuate the hepatic ischemia-reperfusion injury, *Am. J. Transplant.,* 2013, **13**, 409.

13. S. C. Yang, S. H. Chang, P. W. Hsieh, Y. T. Huang, C. M. Ho, Y. F. Tsai, T. L. Hwang, Dipeptide HCH6-1 inhibits neutrophil activation and protects against acute lung injury by blocking FPR1, *Free Radic. Biol. Med*., 2017, **106**, 254.

14. A. L. Stenfeldt, J. Karlsson, C. Wennerås, J. Bylund, H. Fu, C. Dahlgren, Cyclosporin H, Boc-MLF and Boc-FLFLF are antagonists that preferentially inhibit activity triggered through the formyl peptide receptor. *Inflammation*, 2007, **30**, 224.

15. H. L. Rittner, D. Hackel, P. Voigt, S. Mousa, A. Stolz, D. Labuz, M. Schafer, M. Schaefer, C.Stein, A. Brack, Mycobacteria attenuate nociceptive responses by formyl peptide receptor triggered opioid peptide release from neutrophils. *PLoS Pathog.*, 2009, **5**, e1000362.

16. I. A. Schepetkin, A. I. Khlebnikov, M. P. Giovannoni, L. N. Kirpotina, A. Cilibrizzi, M. T. Quinn, Development of small molecule non-peptide formyl peptide receptor (FPR) ligands and molecular modeling of their recognition, *Curr. Med. Chem.,* 2014, **21**, 1478.

17. J. Unitt, M. Fagura, T. Phillips, S. King, M. Perry, A. Morley, C. MacDonald, R. Weaver, J. Christie, S. Barber, R. Mohammed, M. Paul, A. Cook, A. Baxter, Discovery of small molecule human FPR1 receptor antagonists. *Bioorg. Med. Chem. Lett.*, 2011, **21**, 2991.

18. A. D Morley, S. King, B. Roberts, S. Lever, B. Teobald, A. Fisher, T. Cook, B. Parker, M. Wenlock, C. Phillips, K. Grime, Lead optimisation of pyrazoles as novel FPR1 antagonists. *Bioorg. Med.Chem. Lett.,* 2012, **22**, 532.

19. I. A. Schepetkin, L. N. Kirpotina, A. I. Khlebnikov, N. Cheng, R. D. Ye, M. T. Quinn, Antagonism of human formyl peptide receptor 1 (FPR1) by chromones and related isoflavones, *Biochem. Pharmacol.* 2014, **92**, 627.

20. L. N. Kirpotina, I. A. Schepetkin, A. I. Khlebnikov, O. I. Ruban, Y. Ge, R. D. Ye, D. J. Kominsky, M. T. Quinn, 4-Aroyl-3-hydroxy-5-phenyl-1H-pyrrol-2(5H)-ones as N-formyl peptide receptor 1 (FPR1) antagonists, *Biochem Pharmacol.* 2017, **142**, 120.

21. I. A. Schepetkin, A. I. Khlebnikov, L. N. Kirpotina, M. T. Quinn, Antagonism of human formyl peptide receptor 1 with natural compounds and their synthetic derivatives, *Int. Immunopharmacol.* 2016, **37**, 43.

22. P. L. Tsai, J. P. Wang, C. W. Chang, S. C. Kuo, P. D. Chao, Constituents and bioactive principles of Polygonum chinensis, *Phytochemistry*, 1998, **49**, 1663.

23. K. Isshiki, Y. Asai, S. Tanaka, M. Nishio, T. Uchida, T. Okuda, S. Komatsubara, N. Sakurai, Aurantiamide acetate, a selective cathepsin inhibitor, produced by Aspergillus penicilloides, *Biosci. Biotechnol. Biochem.*, 2001, **65**, 1195.

24. X. B. Liu, B. X. Yang, L. Zhang, Y. Z. Lu, M. H. Gong, J. K. Tian, An in vivo and in vitro assessment of the anti-inflammatory, antinociceptive, and immunomodulatory activities of Clematis terniflora DC. extract, participation of aurantiamide acetate, *J. Ethnopharmacol.* 2015, **169**, 287.

25. C. S. Yoon, D. C. Kim, D. S. Lee, K. S. Kim, W. Ko, J. H. Sohn, J. H. Yim, Y. C. Kim, H. Oh, Anti-neuroinflammatory effect of aurantiamide acetate from the marine fungus Aspergillus sp. SF-5921: inhibition of NF-κB and MAPK pathways in lipopolysaccharide-induced mouse BV2 microglial cells, *Int. Immunopharmacol.,* 2014, **23**, 568.

26. T. L. Hwang, C. H. Hung, C. Y. Hsu, Y. T. Huang, Y. C. Tsai, P. W. Hsieh, Design and synthesis of tryptophan containing dipeptide derivatives as formyl peptide receptor 1 antagonist, *Org. Biomol. Chem.,* 2013, **11**, 3742.

27. M. L. Stama, J. Ślusarczyk, E. Lacivita, L. N. Kirpotina, I. A. Schepetkin, K. Chamera, C. Riganti, R. Perrone, M. T. Quinn, A. Basta-Kaim, M. Leopoldo, Novel ureidopropanamide based

N-formyl peptide receptor 2 (FPR2) agonists with potential application for central nervous system disorders characterized by neuroinflammation. *Eur. J. Med Chem.,* 2017, **141**, 703.

28. J. S. Mills, H. M. Miettinen, D. Cummings, A. J. Jesaitis, Characterization of the binding site on the formyl peptide receptor using three receptor mutants and analogs of Met-Leu-Phe and Met-Met-Trp-Leu-Leu, *J. Biol .Chem.,* 2000, **275**, 39012.

29. C. K. Derian, H. F. Solomon, J. D. Higgins 3rd, M. J. Beblavy, R. J. Santulli, G. J. Bridger, M. C. Pike, D. J. Kroon, A. J. Fischman, Selective inhibition of N-formylpeptide-induced neutrophil activation by carbamate-modified peptide analogues, *Biochemistry*, 1996, **35**, 1265.

Figure 1. “Small-molecule” FPR1 antagonists

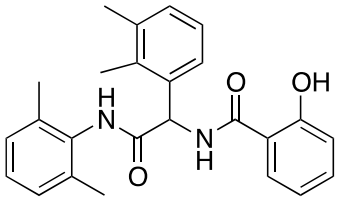

1

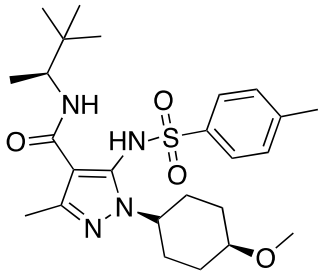

2

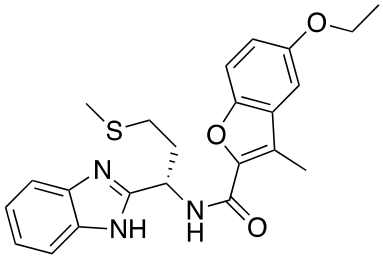

3

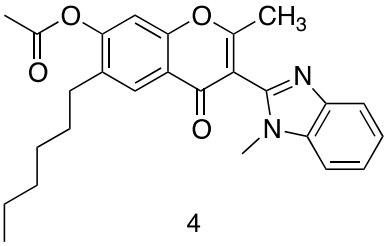

4

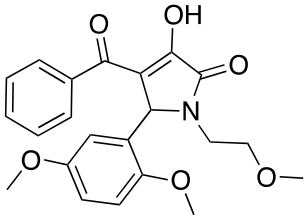

5

Figure 2. Aurantiamide acetate and structurally related FPR1 Antagonists.

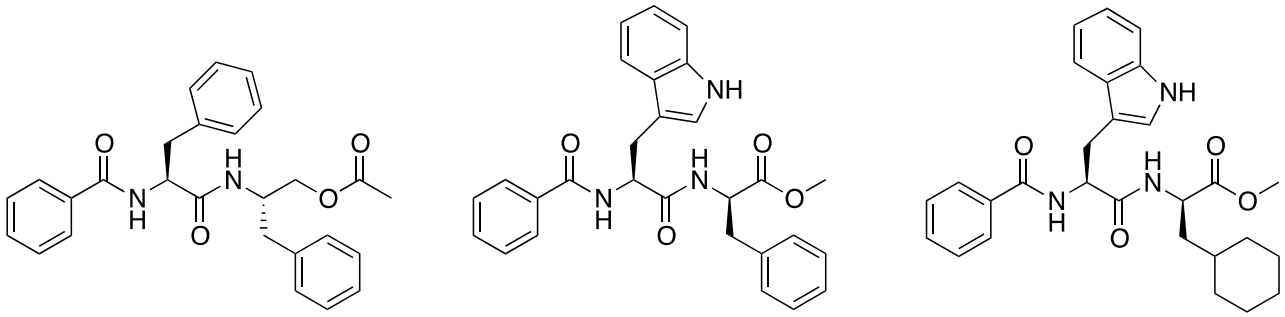

aurantiamide acetate (2R,2'S)-6 (2R,2'S)-7

Table 1. Effect of the four stereoisomers of compound **6** and (2*R*,2'*S*)-**7** on Ca^{2+} mobilization in FPR1- and FPR2-HL60 transfected cells and human neutrophils.

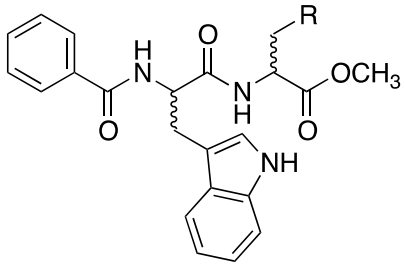

		FPR1-HL60 Cells		FPR2-HL60 Cells		Neutrophils	
Compd.	**R**	**EC_{50}, μM**	**IC_{50}, μM**	**EC_{50}, μM**	**IC_{50}, μM**	**EC_{50}, μM**	**IC_{50}, μM**
(2*R*,2'*S*)-**6**	Ph	N.A.[a]	0.45 ± 0.1	N.A.	N.A.	N.A.	0.18 ± 0.11
(2*R*,2'*S*)-**7**	Cyclohexyl	N.A.	0.67 ± 0.1	N.A.	N.A.	N.A.	0.12 ± 0.09
(2*S*,2'*R*)-**6**	Ph	N.A.	37.4 ± 9.7	N.A.	N.A.	N.A.	10.9 ± 2.1
(2*S*,2'*S*)-**6**	Ph	N.A.	5.8 ± 0.25	N.A.	12.3 ± 0.8	N.A.	2.4 ± 0.4
(2*R*,2'*R*)-**6**	Ph	N.A.	16.5 ± 0.8	N.A.	N.A.	N.A.	31.3 ± 9.2

[a]Not Active

Table 2. Effect of compounds **10-13** and (2*R*,2'*S*)-**8** on Ca^{2+} mobilization in FPR1- and FPR2-HL60 transfected cells and human neutrophils.

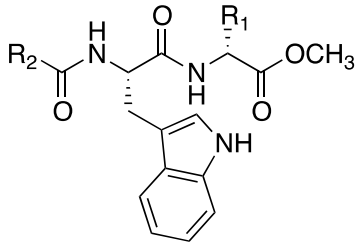

			FPR1-HL60 Cells		FPR2-HL60 Cells		Neutrophils	
Compd.	**R_1**	**R_2**	**EC_{50}, μM**	**IC_{50}, μM**	**EC_{50}, μM**	**IC_{50}, μM**	**EC_{50}, μM**	**IC_{50}, μM**
10	CH_2Ph	cyclohexyl	N.A.[a]	0.54 ± 0.17	N.A.	N.A.	N.A.	3.3 ± 0.4
11	CH_2Ph	$CH_2CH(CH_3)_2$	N.A.	19.6 ± 4.2	N.A.	N.A.	N.A.	27.7 ± 6.3
(2*R*,2'*S*)-**8**	CH_2Ph	$OC(CH_3)_3$	N.A.	17.1 ± 3.6	10.5 ± 2.0	N.A.	N.A.	12.6 ± 2.8
12	$CH_2CH(CH_3)_2$	Ph	N.A.	24.7 ± 4.3	10.9 ± 3.2	N.A.	N.A.	14.5 ± 4.5
13	$CH(CH_3)_2$	Ph	N.A.	11.7 ± 2.8	N.A.	N.A.	N.A.	25.3 ± 7.1

[a]Not Active

Table 3. Effect of compounds (2*R*, 2'*S*)-**6**, (2*R*, 2'*S*)-**7**, (2*S*, 2'*S*)-**6**, and **10** on neutrophils chemotaxis.

Compd.	**Neutrophils chemotaxis inhibition IC_{50}, μM**
2*R*, 2'*S*)-**6**	0.48 ± 0.03
(2*R*, 2'*S*)-**7**	0.62 ± 0.31
(2*S*, 2'*S*)-**6**	1.6 ± 0.59
10	3.1 ± 0.7

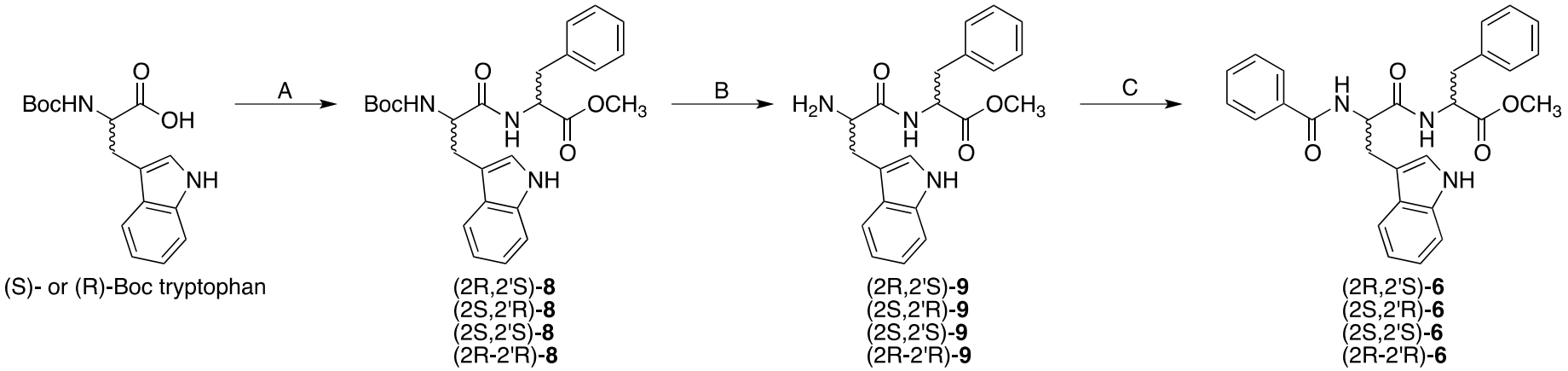

Scheme 1. Reagents and conditions: (A) *N-N'*-carbonyldiimidazole, (S)- or (R)-phenylalanine methyl ester, anhydrous THF, r.t., 24 h, 41-75% yield; (B) TFA, CH_2Cl_2, r.t., 5 h, quantitative yield; (C) benzoic acid, *N-N'*-carbonyldiimidazole, anhydrous THF, r.t., 24 h, 21-50% yield.

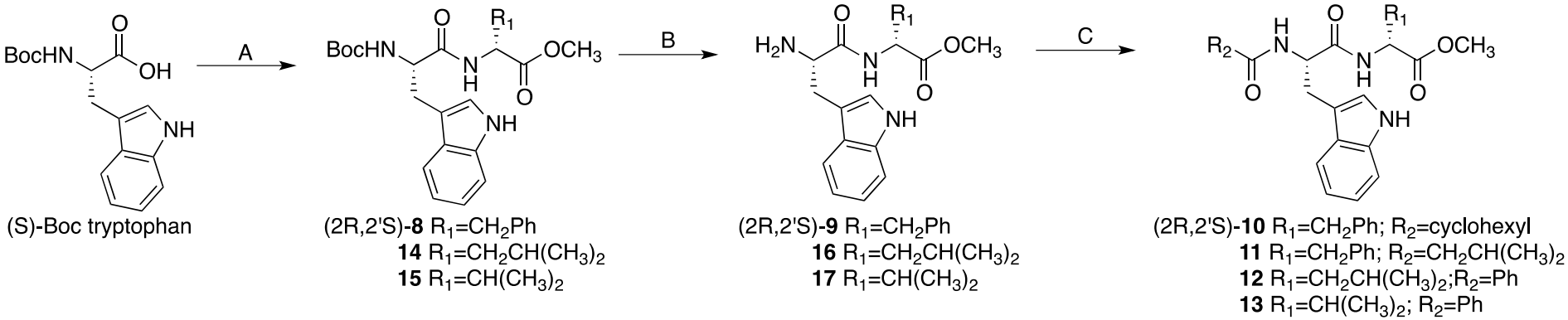

Scheme 2. Reagents and conditions: (A) (*R*)-aminoacid methyl ester, *N-N'*-carbonyldiimidazole, anhydrous THF, r.t., 24 h, 41-71% yield; or (*R*)-valine methyl ester, PyBOP and N-methylmorpholine, DMF, r.t., overnight, 77% yield; (B) TFA, CH_2Cl_2, r.t., 5 h, quantitative yield; (C) carboxylic acid, *N-N'*-carbonyldiimidazole, anhydrous THF, r.t., 24 h, 15-23% yield.

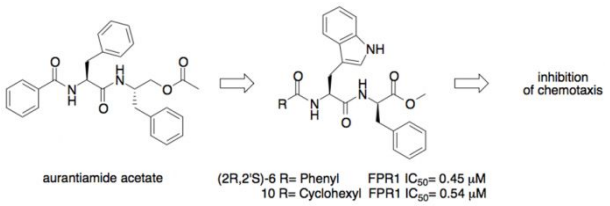

Aurantiamide is a useful scaffold to develop promising FPR1 antagonists capable to inhibit neutrophils chemotaxis.